Multiple Additions of Vaska-Type Iridium Complexes to C_{60}. Preferential Crystallization of the "Para" Double Addition Products $C_{60}\{Ir(CO)Cl(PMe_3)_2\}_2 \cdot 2C_6H_6$ and $C_{60}\{Ir(CO)Cl(PEt_3)_2\}_2 \cdot C_6H_6$

Alan L. Balch,* Joong W. Lee, Bruce C. Noll, and Marilyn M. Olmstead

Department of Chemistry, University of California, Davis, California 95616

Received May 25, 1994[⊗]

Factors responsible for the crystallization of multiple addition products of C_{60} with Vaska-type iridium complexes have been examined. A 10-fold excess of $Ir(CO)Cl(PMe_3)_2$ reacted with a benzene solution of C_{60} over a period of 7 days to give the double addition product, $C_{60}\{Ir(CO)Cl(PMe_3)_2\}_2 \cdot 2C_6H_6$. Black parallelepipeds form in the orthorhombic space group *Cmcm* (No. 63) with $a = 20.188(4)$ Å, $b = 16.042(3)$ Å, and $c = 18.517(4)$ Å, at 123 K with $Z = 4$. Refinement (on F^2) of 3641 reflections and 225 parameters with 73 restraints yielded $R = 0.065$ (for 2506 reflections with $I > 2.0\,\sigma(I)$) and w$R2 = 0.142$. Reaction of a 10-fold excess of $Ir(CO)Cl(PEt_3)_2$ with a saturated benzene solution of C_{60} resulted in the gradual formation of yet another crystalline double addition product, $C_{60}\{Ir(CO)Cl(PEt_3)_2\}_2 \cdot C_6H_6$. Black needles form in the monoclinic space group *I2/a* (an alternate setting of No. 15) with $a = 20.105(2)$ Å, $b = 12.467(1)$ Å, $c = 26.458(2)$ Å, $\beta = 99.63(1)°$ at 123 K with $Z = 4$. Refinement (on F^2) of 4275 reflections and 242 parameters with 42 restraints yielded $R = 0.073$ for 3987 reflections with $I > 2.0\sigma(I)$ and w$R2 = 0.190$. Both double addition products have the iridium complexes bound as usual to 6:6 ring junctions. Both also have the two complexes bound at the "para" positions at opposite ends of the fullerene. As a result of the distortions induced by the binding of the two iridium complexes, the fullerene portion is elongated by 0.40 Å along the Ir---Ir axis. $^{31}P\{^1H\}$ NMR and infrared spectroscopic studies of solution of $C_{60}\{Ir(CO)Cl(PEt_3)_2\}_2 \cdot C_6H_6$ in 6:4 *o*-dichlorobenzene/toluene indicate that there is extensive dissociation of the adducts at room temperature. At −80 °C there is evidence of the formation of a multiplicity of adducts which are probably the regioisomers of the double addition product. We believe that isolation of the "para" double addition products is a consequence of the low solubility of this isomer which possesses the lowest polarity and highest symmetry of all of the possible eight regioisomers of these double addition products.

Introduction

Addition reactions to the 6:6 ring junctions of C_{60} are a prominent feature of fullerene chemistry.[1] As a result of the high symmetry of C_{60} and the presence of 30 individual 6:6 ring junctions, there is the possibility of forming a variety of adducts which differ in level of addition and/or in geometry. Varying levels of addition are observed, for example, in the case of the reaction of C_{60} with diethyl bromomalonate and sodium hydride, where $C_{60}\{C(COOEt)_2\}_n$ compounds with $n = 1$, 2, and 3 are formed,[2] and with the addition of $Pt(PR_3)_2$, where the single- and hexa-addition products, $C_{60}\{Pt(PR_3)_2\}$ and $C_{60}\{Pt(PR_3)_2\}_6$, have been structurally characterized and intermediate levels of addition reported.[3,4] Regioisomers can form at each level of addition. For example, double addition to C_{60} at 6:6 ring junctions allows eight regioisomers to form as demonstrated in Figure 1. As this figure shows, if the first addition occurs at the arrow, then one product, the "para" isomer (**1**) with maximal D_{2h} symmetry, along with four isomers (**4**, **5**, **7**, **8**) with maximal C_s symmetry and three isomers (**2**, **3**, **6**) with maximal C_2 symmetry, can form.

The addition of Vaska-type iridium complexes, $Ir(CO)Cl(PR_3)_2$, to fullerenes has proven to be an effective way of obtaining materials that are suitable for study by single-crystal X-ray diffraction. This procedure has produced detailed structural information on the higher fullerenes, C_{70}[5] and C_{84},[6] and on the fullerene epoxide, $C_{60}O$[7], as well as on C_{60} itself.[8,9] The reactivity of the iridium complexes that are involved in these addition reactions can be altered by changing the ligands. Increasing the basicity of the phosphine ligands results in iridium complexes that are more prone to addition reactions of this

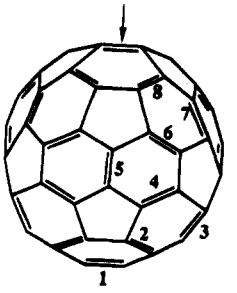

Site	Max. Symm.
8	C_s
7	C_s
6	C_2
5	C_s
4	C_s
3	C_2
2	C_2
1	D_{2h}

Figure 1. Sites for double addition to C_{60}. The initial addition is presumed to occur at the arrow and the numbers **1-8** identify the possible isomers. The maximum symmetry given in the table results when the added group has C_{2v} symmetry. With Vaska- type complexes as the added groups, the symmetry of the adducts is lower because of the inequivalence of the carbonyl and chloro groups.

[⊗] Abstract published in *Advance ACS Abstracts,* October 1, 1994.

(1) Taylor, R.; Walton, D. R. M. *Nature* **1993**, *363*, 685. Fagan, P. J.; Chase, B.; Calabrese, J. C.; Dixon, D. A.; Harlow, R.; Krusic, P. J.; Matsuzawa, N.; Tebbe, F. N.; Thorn, D. L.; Wasserman, E. *Carbon* **1992**, *30*, 1213.
(2) Hirsch, A.; Lamparth, I.; Karfunkel, H. R. *Angew. Chem., Int. Ed. Engl.* **1994**, *33*, 437.
(3) Fagan, P. J.; Calabrese, J. C.; Malone, B. *Science* **1991**, *252*, 1160.
(4) Fagan, P. J.; Calabrese, J. C.; Malone, B. *J. Am. Chem. Soc.* **1991**, *113*, 9408.
(5) Balch, A. L.; Catalano, V. J.; Lee, J. W.; Olmstead, M. M.; Parkin, S. R. *J. Am. Chem. Soc.* **1991**, *113*, 8953.
(6) Balch, A. L.; Ginwalla, A. S.; Lee, J. W.; Noll, B. C.; Olmstead, M. M. *J. Am. Chem. Soc.* **1994**, *116*, 2227.
(7) Balch, A. L.; Catalano, V. J.; Lee, J. W. *Inorg. Chem.* **1991**, *30*, 3980.
(8) Balch, A. L.; Catalano, V. J.; Lee, J. W.; Olmstead, M. M. *J. Am. Chem. Soc.* **1992**, *114*, 5455.

0020-1669/94/1333-5238$04.50/0

type.[10] While the addition of $Ir(CO)Cl(PPh_3)_2$ to C_{60} produces only the monoaddition product, $(\eta^2\text{-}C_{60})Ir(CO)Cl(PPh_3)_2$, addition of the more reactive complex $Ir(CO)Cl(PMe_2Ph)_2$ to C_{60} produces a mixture of four solids: well-formed, purple-black obelisks, $C_{60}\{Ir(CO)Cl(PMe_2Ph)_2\}_2{\cdot}C_6H_6$; small purple-black plates, $C_{60}\{Ir(CO)Cl(PMe_2Ph)_2\}_2{\cdot}2C_6H_6$; clumps of needles, which are presumed to be the single addition product; and an apparently amorphous material.[11] The two double addition products have been characterized by single crystal X-ray diffraction. Both have the iridium complexes bound to opposite poles of the fullerene in a "para" fashion. As usual, the iridium atoms are coordinated to the fullerene in η^2-fashion at 6:6 ring junctions. These two double addition products differ in the amount of benzene that cocrystallizes with the fullerene adducts and in the disposition of the phenyl substituents on the phosphine ligands. In the obelisks, the four phenyl groups are oriented over the fullerene and make face-to-face $\pi-\pi$ contacts with it. However, in the small purple plates, all four phenyl groups are directed away from the fullerene and there is no $\pi-\pi$ contact between these moieties.

Here we report on the formation of double addition products of C_{60} with $Ir(CO)Cl(PMe_3)_2$ and $Ir(CO)Cl(PEt_3)_2$. This work was undertaken with the initial goal of forming adducts with three or more Vaska-type complexes bound to the exterior of C_{60}. The smaller bulk and higher chemical reactivity of these two iridium complexes were believed to be useful in forming multiple addition products. However, only double addition products with a "para" arrangement were obtained in crystalline form.

Results

The reaction of C_{60}, which forms purple solutions, with a 10-fold excess of either $Ir(CO)Cl(PMe_3)_2$ or $Ir(CO)Cl(PEt_3)_2$ in benzene produces green solutions. The formation of this green color indicates that reaction between the two components to form one or more adducts has occurred almost immediately upon mixing. When these solutions are allowed to stand undisturbed for 7 days, purple/black crystals deposit. The infrared spectra of the products show the increase in the carbon monoxide stretching frequency that is expected for such adducts.[5-9,11,12] For the starting materials, $Ir(CO)Cl(PMe_3)_2$ and $Ir(CO)Cl(PEt_3)_2$, $\nu(C\equiv O)$ is 1952 and 1947 cm^{-1} (in a fluorocarbon mull), respectively. The products each display a single $\nu(C\equiv O)$ at 2000 cm^{-1} for $C_{60}\{Ir(CO)Cl(PMe_3)_2\}_2{\cdot}2C_6H_6$ and at 2001 cm^{-1} for $C_{60}\{Ir(CO)Cl(PEt_3)_2\}_2{\cdot}C_6H_6$. These two sets of crystalline adducts have been examined by X-ray diffraction. In both cases microscopic examination of the product indicated that it was homogeneous. The range of crystal shapes seen for the product of the $C_{60}/Ir(CO)Cl(PMe_2Ph)_2$ reaction[11] was not observed for either product. For each adduct, a number of different crystals were examined by X-ray diffraction and all possessed a common set of cell dimensions.

The Structure of $C_{60}\{Ir(CO)Cl(PMe_3)_2\}_2{\cdot}2C_6H_6$. Table 1 contains the atomic coordinates, while Table 2 contains selected interatomic distances and angles. A view of the molecule is shown in Figure 2. The molecule is positioned at a site of crystallographic $2/m$ (C_{2h}) symmetry. The C_2 axis passes through the two iridium atoms, while the mirror plane bisects the fullerene midway between these two metal atoms. As usual the iridium atoms are bound to the fullerene at 6:6 ring junctions. Molecular dimensions within this molecule are unexceptional. As is frequently observed in complexes that contain the *trans*-Cl−Ir−CO group,[5,13] there is disorder in the position of the carbonyl and chloride ligands which interchanges their relative

Table 1. Atomic Coordinates ($\times 10^4$) and Equivalent Isotropic Displacement Parameters ($Å^2 \times 10^3$) for $\eta^2\text{-}C_{60}\{Ir(CO)Cl(PMe_3)_2\}_2{\cdot}2C_6H_6$

	x	y	z	U(eq)[a]
Ir	2177(1)	2198(1)	7500	14(1)
P	1483(1)	2229(2)	6493(1)	22(1)
Cl	2152(3)	3676(2)	7500	21(1)
Cl′	2154(10)	728(3)	7500	21(1)
O	2050(7)	344(6)	7500	32(3)
O′	2040(29)	4027(19)	7500	32(3)
C(1)	3185(4)	2213(6)	7093(5)	15(2)
C(2)	3487(4)	1491(6)	6729(5)	14(2)
C(3)	3861(5)	1754(6)	6107(5)	16(2)
C(4)	3869(5)	2663(6)	6112(5)	17(2)
C(5)	3492(4)	2935(6)	6726(5)	15(2)
C(6)	3719(4)	778(6)	7100(5)	17(2)
C(7)	4299(4)	336(6)	6849(5)	15(2)
C(8)	4640(4)	594(7)	6250(6)	21(2)
C(9)	4420(5)	1321(7)	5858(6)	22(2)
C(10)	5000	1779(9)	5623(8)	17(3)
C(11)	5000	2644(10)	5620(8)	23(3)
C(12)	4418(5)	3089(6)	5868(5)	14(2)
C(13)	4637(4)	3817(6)	6248(5)	19(2)
C(14)	4294(4)	4075(6)	6863(5)	15(2)
C(15)	3703(4)	3623(6)	7099(5)	19(2)
C(16)	4657(6)	4356(9)	7500	20(3)
C(17)	4651(6)	62(8)	7500	17(3)
C(18)	2136(10)	1048(5)	7500	12(3)
C(18′)	2177(42)	3338(6)	7500	12(3)
C(19)	1942(6)	2250(9)	5674(6)	38(3)
C(20)	944(5)	1336(7)	6374(7)	37(3)
C(21)	941(7)	3124(8)	6406(8)	48(4)
C(1S)	1871(8)	−176(10)	9656(6)	28(2)
C(2S)	2468(9)	−325(12)	9305(9)	28(2)
C(3S)	3053(8)	−167(10)	9655(6)	28(2)
C(1B)	1763(14)	0	10000	28(2)
C(2B)	2111(10)	−259(14)	9388(11)	28(2)
C(3B)	2789(10)	−252(14)	9389(11)	28(2)
C(4B)	3138(14)	0	10000	28(2)

[a] U(eq) is defined as one-third of the trace of the orthogonalized U_{ij} tensor. C(1S)−C(4B) are the carbon atoms of the solvate benzene molecules.

Table 2. Selected Interatomic Distances and Angles for the "Para" Fullerene Adducts

	$C_{60}\{Ir(CO)Cl(PMe_3)_2\}_2{\cdot}2C_6H_6$	$C_{60}\{Ir(CO)Cl(PEt_3)_2\}_2{\cdot}C_6H_6$
	Lengths (Å)	
Ir−C(1)	2.169(8)	2.202(11)
Ir−C(2)		2.178(12)
Ir−P(1)	2.333(3)	2.355(4)
Ir−P(2)		2.365(4)
Ir−Cl	2.372(3)	2.407(3)
Ir−C(18 or 31)	1.846(8)	1.80(2)
Ir- - -Ir	11.398(2)	11.427(2)
C(1)−C(1)′ or C(2)	1.51(2)	1.49(2)
	Angles (deg)	
C(1)−Ir−C(1′ or 2)	40.6(5)	39.8(4)
P(1)−Ir−P(1′ or 2)	106.17(13)	106.8(2)
Cl−Ir−P(1)	88.64(12)	87.66(14)
Cl−Ir−P(2)		86.69(14)
Cl−Ir−C(18 or 31)	176.2(7)	177.7(6)
Cl−Ir−C(1)	90.5(3)	90.5(3)
Cl−Ir−C(2)		90.8(3)

(9) Deeming, A. J.; Shaw, B. L. *J. Chem. Soc. A* **1969**, 1802.
(10) Balch, A. L.; Lee, J. W.; Noll, B. C.; Olmstead, M. M. *J. Am. Chem. Soc.* **1992**, *114*, 10984.
(11) Balch, A. L.; Costa, D. L.; Lee, J. W.; Noll, B. C.; Olmstead, M. M. *Inorg. Chem.* **1994**, *33*, 2071.
(12) Vaska, L. *Acc. Chem. Res.* **1968**, *1*, 335.
(13) Churchill, M. R.; Fettinger, J. C.; Buttrey, L. A.; Barkan, M. D.; Thomson, J. S. *J. Organomet. Chem.* **1988**, *340*, 257.

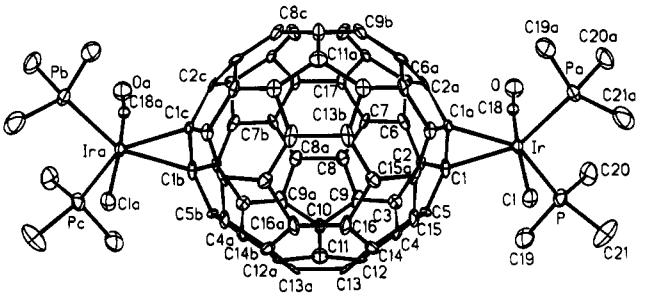

Figure 2. Perspective view of $C_{60}\{Ir(CO)Cl(PMe_3)_2\}_2{\cdot}2C_6H_6$ with 50% thermal contours for all atoms.

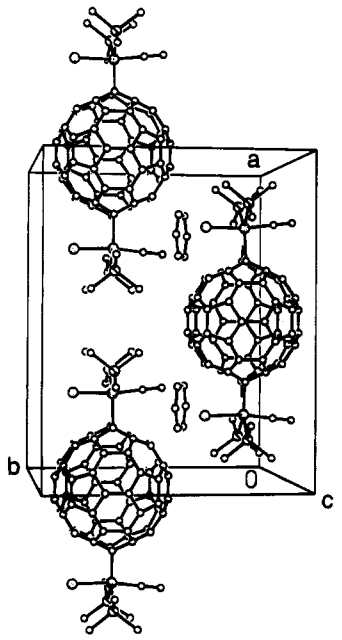

Figure 3. View of the packing in solid $C_{60}\{Ir(CO)Cl(PMe_3)_2\}_2{\cdot}2C_6H_6$.

locations. The figure shows only the location of these ligands within the major form, which has 0.78 fractional occupancy.

The fullerene portion of the molecule is distorted by the binding of the iridium complexes. These complexes pull the two carbon atoms to which they are bound out from the fullerene core.[8] Since the two iridium complexes are located opposite one another, the distortion results in a marked elongation of the fullerene along the Ir---Ir axis. The distance between the midpoints of the C(1)−C(1a) and C(1b)−C(1c) bonds is 7.330 Å. In comparison the dimensions in the two orthogonal directions that are perpendicular to this axis are shorter. The distance between the midpoints of the C(16)−C(16a) and C(17)−C(17a) bonds is 6.888 Å, and the distance between the midpoints of the C(10)−C(11) and the C(10a)−C(11a) bonds is 6.957 Å. In comparison, the corresponding distance in free C_{60} is 6.938 Å.[14]

A view of the packing of the molecules in the solid state is shown in Figure 3. Columns of the fullerene complexes are formed. These columns are oriented parallel to the *a* axis. The intermolecular contacts along these columns involve the methyl groups on the periphery of the adducts. As the figure shows, the coordinated $Ir(CO)Cl(PMe_3)_2$ units and the C_{60} have similar external dimensions about the column axis. Benzene molecules fill the channels between these columns. These benzene molecules are disordered over two nearly coplanar orientations that are related by a 30° rotation through the normal that passes through the center of each benzene ring. They do not make $\pi-\pi$ contact with the fullerene but appear to merely fill what would otherwise be voids in the solid.

(14) This is the average of nine independant distances in the ordered structure of $C_{60}{\cdot}2SbPh_3$: Olmstead, M. M.; Fedurco, M.; Fawcett, W. R. To be published.

Table 3. Atomic Coordinates ($\times 10^4$) and Equivalent Isotropic Displacement Parameters ($Å^2 \times 10^3$) for $C_{60}\{Ir(CO)Cl(PEt_3)_2\}_2{\cdot}C_6H_6$

	x	*y*	*z*	*U*(eq)[a]
Ir	4960(1)	3370(1)	6458(1)	27(1)
Cl	4984(1)	2121(2)	7155(1)	23(1)
O	4923(9)	4972(14)	5639(7)	103(5)
P(1)	5898(3)	4221(4)	6947(2)	69(2)
P(2)	3989(2)	4112(4)	6719(2)	58(1)
C(1)	5357(6)	2129(9)	5996(4)	20(3)
C(2)	4604(6)	2118(9)	5905(4)	21(3)
C(3)	4261(6)	2387(10)	5377(5)	24(3)
C(4)	4605(6)	2769(10)	5001(4)	23(3)
C(5)	5347(6)	2786(9)	5098(4)	21(3)
C(6)	5693(6)	2417(9)	5567(4)	22(3)
C(7)	6277(6)	1757(9)	5569(5)	22(3)
C(8)	6507(6)	1506(9)	5118(5)	24(3)
C(9)	6152(6)	1882(10)	4631(5)	25(3)
C(10)	5565(6)	2497(10)	4625(4)	23(3)
C(11)	4978(6)	2308(9)	4238(4)	20(3)
C(12)	4995(6)	1494(9)	3881(4)	18(2)
C(13)	5592(5)	847(9)	3885(4)	16(2)
C(14)	6162(6)	1046(9)	4253(4)	22(3)
C(15)	6529(6)	137(9)	4504(4)	22(3)
C(16)	6750(6)	425(10)	5038(5)	25(3)
C(17)	3681(6)	1704(9)	5225(5)	21(3)
C(18)	3459(6)	1446(10)	4721(5)	25(3)
C(19)	3821(6)	1837(10)	4326(5)	25(3)
C(20)	4391(6)	2480(9)	4473(4)	23(3)
C(21)	3243(6)	342(10)	4580(5)	25(3)
C(22)	3476(6)	69(9)	4106(4)	22(3)
C(23)	3838(6)	991(9)	3949(4)	18(2)
C(24)	4415(5)	836(9)	3733(4)	15(2)
C(25)	4644(5)	−255(8)	3651(4)	12(2)
C(26)	5375(6)	−232(9)	3743(4)	17(2)
C(27)	3684(6)	907(9)	5628(4)	22(3)
C(28)	4267(6)	1097(9)	6018(4)	17(2)
C(29)	5705(5)	1128(9)	6205(4)	16(2)
C(30)	6281(6)	955(9)	5965(4)	20(3)
C(31)	4962(10)	4344(16)	5954(8)	64(5)
C(32)	5723(12)	5696(15)	6768(11)	38(2)
C(33)	6276(10)	6415(15)	6850(8)	75(6)
C(34)	6660(11)	3882(17)	6733(9)	38(2)
C(35)	6838(12)	2775(16)	6969(10)	38(2)
C(36)	5952(7)	4338(11)	7629(5)	30(3)
C(37)	6599(7)	4720(11)	7943(5)	35(3)
C(38)	3265(10)	2817(16)	6706(7)	38(2)
C(39)	2861(14)	2697(24)	6279(10)	109(9)
C(40)	4039(6)	4472(10)	7380(5)	27(3)
C(41)	3387(7)	4818(11)	7557(5)	34(3)
C(42)	3441(10)	5086(14)	6351(8)	38(2)
C(43)	3779(12)	6176(14)	6422(9)	38(2)
C(44)	2500	3906(17)	5000	37(5)
C(45)	1987(7)	4471(10)	5166(5)	29(3)
C(46)	1977(7)	5570(11)	5166(5)	34(3)
C(47)	2500	6125(18)	5000	43(5)
C(32′)	6463(13)	5245(17)	6759(11)	38(2)
C(34′)	6600(14)	3112(23)	7097(11)	38(2)
C(35′)	7015(14)	3037(25)	6689(12)	38(2)
C(38′)	3211(18)	3686(42)	6347(18)	38(2)
C(42′)	4080(17)	5512(20)	6447(14)	38(2)
C(43′)	3508(20)	6215(22)	6514(16)	38(2)

[a] *U*(eq) is defined as one-third of the trace of the orthogonalized U_{ij} tensor.

Structure of $C_{60}\{Ir(CO)Cl(PEt_3)_2\}_2{\cdot}C_6H_6$. Atomic coordinates are presented in Table 3. A selection of interatomic distances and angles is given in Table 2, where they may be compared to those of $C_{60}\{Ir(CO)Cl(PMe_3)_2\}_2{\cdot}2C_6H_6$. A drawing of the molecule is given in Figure 4. The molecule is located on a crystallographic center of symmetry.

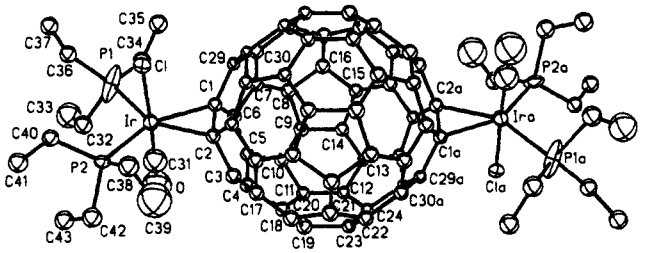

Figure 4. Perspective view of $C_{60}\{Ir(CO)Cl(PEt_3)_2\}_2 \cdot C_6H_6$ with 50% thermal contours for all atoms.

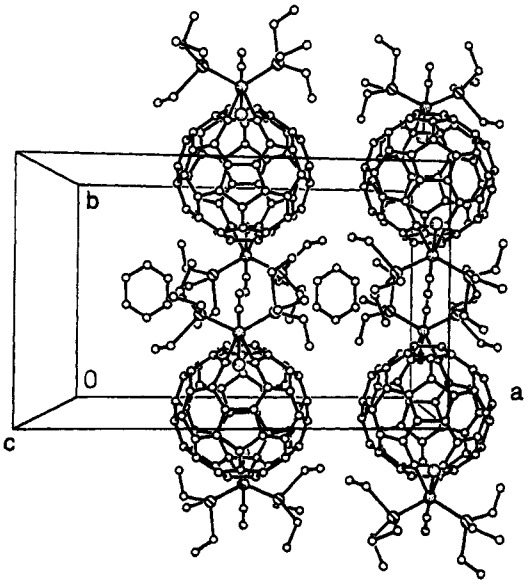

Figure 5. View of the packing in solid $C_{60}\{Ir(CO)Cl(PEt_3)_2\}_2 \cdot C_6H_6$.

The geometry of the molecule with the two iridium atoms located in the "para" position is similar to that of the trimethylphosphine analog. The size of the thermal ellipsoids for the carbonyl and chloride ligands suggests that there may be some disorder in these groups, but this is too small to adequately resolve. The ethyl groups also display a degree of disorder. Only the major orientations of these side chains are shown in Figure 4.

The fullerene portion shows the same sort of distortion as that seen in $C_{60}\{Ir(CO)Cl(PMe_3)_2\}_2 \cdot 2C_6H_6$. Thus, the distance between the midpoints of the C(1)–C(2) and C(1a)–C(2a) bonds (the distance along the Ir–Ir axis) is 7.312 Å, while the distances between the midpoints of the C(16)–C(21a) and the C(16a)–C(21) bonds is 6.952 Å, and the distance between the midpoints of the C(11)–C(12) and the C(11a)–C(12a) bonds is 6.868 Å.

A view of the packing in the solid state is shown in Figure 5. Comparison with Figure 2 shows that there are major differences in the way the molecules are arranged in the two solids. Nevertheless, the fullerene complexes again form columns that run parallel to the *a* axis, but here each successive member is rotated by 90°, and direct fullerene–fullerene contacts occur along the axis of the column. The fullerene–fullerene center-to-center separation in these columns is 10.052 Å. The ligands on the iridium atoms protrude into the spaces between these columns. The benzene molecules are also found in the spaces between two columns, where they again occupy sites that would otherwise represent voids in the solid.

Solution Behavior of $C_{60}\{Ir(CO)Cl(PEt_3)_2\}_2 \cdot C_6H_6$. While the solids, $C_{60}\{Ir(CO)Cl(PMe_3)_2\}_2 \cdot 2C_6H_6$ and $C_{60}\{Ir(CO)Cl(PEt_3)_2\}_2 \cdot C_6H_6$, have essentially negligible ability to redissolve in benzene, $C_{60}\{Ir(CO)Cl(PEt_3)_2\}_2 \cdot C_6H_6$ does dissolve in *o*-dichlorobenzene. We found that a 6:4 *o*-dichlorobenzene/toluene mixture was capable of dissolving a sufficient amount of the adduct for ^{31}P NMR study. Moreover, this solvent mixture had a sufficiently large liquid range so that we were able to examine the spectrum at temperatures as low as −80 °C, far below the freezing point of *o*-dichlorobenzene (−18 °C). In this solvent mixture, the $^{31}P\{^1H\}$ NMR spectrum of $Ir(CO)Cl(PEt_3)_2$ consists of a narrow singlet at 20.2 ppm at 20 °C. Relevant $^{31}P\{^1H\}$ NMR spectra for solutions of $C_{60}\{Ir(CO)Cl(PEt_3)_2\}_2 \cdot C_6H_6$ are shown in Figure 6. Trace A shows the spectrum at 20 °C where two very broad resonances are present. The relative intensity ratio between the low-field and high-field resonances is 1.9. Trace B shows the spectrum of the sample after cooling to −30 °C. The two lines have sharpened considerably, the upfield line shows asymmetry, and the ratio of relative intensities of the low field to high-field resonances has changed to 0.4. Trace C shows the spectrum that was obtained after cooling the sample to −80 °C. Further narrowing of all resonances has occurred, and the upfield resonance is now comprised of at least 16 individual components. At this temperature, the ratio of intensities between the resonance at 20.8 ppm and the group of resonances at ca. −18 ppm is 0.15. Addition of an excess of C_{60} to this sample gives the $^{31}P\{^1H\}$ NMR spectrum shown in trace D. Only a single resonance is observed.

These data are consistent with extensive dissociation of the adduct in solution as shown in eqs 1 and 2. The resonance at

$$C_{60}\{Ir(CO)Cl(PEt_3)_2\}_2 \rightleftharpoons C_{60}\{Ir(CO)Cl(PEt_3)_2\} + Ir(CO)Cl(PEt_3)_2 \quad (1)$$

$$C_{60}\{Ir(CO)Cl(PEt_3)_2\} \rightleftharpoons C_{60} + Ir(CO)Cl(PEt_3)_2 \quad (2)$$

ca. 20.8 ppm is readily assigned to free $Ir(CO)Cl(PEt_3)_2$. The broadening seen at 20 °C in trace A is readily explained by rapid exchange of the free- and fullerene-bound iridium complexes. The single line seen in trace D can be assigned to the single addition product $C_{60}\{Ir(CO)Cl(PEt_3)_2\}$ which forms in the presence of excess C_{60} through the reverse of reaction 2 and by reaction 3. The multiplicity of lines in the −16 to −20

$$C_{60}\{Ir(CO)Cl(PEt_3)_2\}_2 + C_{60} \rightleftharpoons 2C_{60}\{Ir(CO)Cl(PEt_3)_2\} \quad (3)$$

ppm region can be understood if a variety of isomeric forms of the double addition product (and possibly some higher addition products) are present. There are seven other isomeric double addition products in addition to the "para" isomer which may form. Because of their lower symmetry and the presence of inequivalent phosphorus atoms, each of these seven regioisomers could produce at least two ^{31}P NMR resonances. Thus the observed multiplicity of resonances is not hard to explain.

Cooling the sample results in alteration of the ratio of the amounts of free- and fullerene- coordinated $Ir(CO)Cl(PEt_3)_2$ that are present. At room temperature, free $Ir(CO)Cl(PEt_3)_2$ is prevalent while, at −80 °C, the fullerene-coordinated form is dominant. This behavior is consistent with thermodynamic considerations in which the entropically driven dissociation is more significant at higher temperatures.

The infrared spectrum obtained from a *o*-dichlorobenzene/toluene solution of $C_{60}\{Ir(CO)Cl(PEt_3)_2\}_2 \cdot C_6H_6$ at 23 °C is also consistent with extensive dissociation. Two bands are observed in the carbon monoxide stretching region: one at 1941 cm^{-1} which is identical to that observed when $Ir(CO)Cl(PEt_3)_2$ is dissolved in this solvent mixture and one of about half the

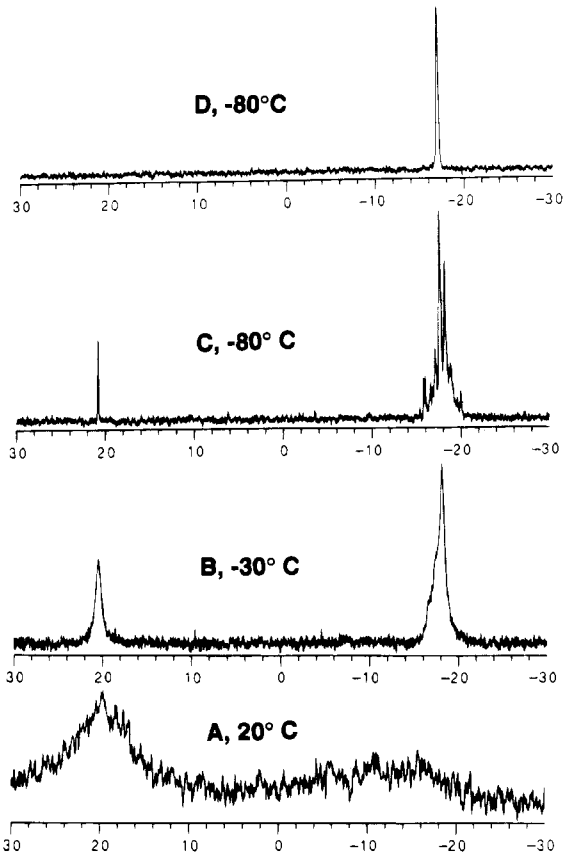

Figure 6. 121 MHz $^{31}P\{^1H\}$ NMR spectra of $C_{60}\{Ir(CO)Cl(PEt_3)_2\}_2{\cdot}C_6H_6$ dissolved in 6:4 v/v mixture of *o*-dichlorobenzene and toluene at (A) 20 °C, (B) −30 °C, (C) −80 °C, and (D) −80 °C after the addition of excess C_{60}.

intensity at 2002 cm^{-1} which is due to the fullerene adduct, $C_{60}\{Ir(CO)Cl(PEt_3)_2\}$.

Discussion

Two new double addition products of C_{60} with Vaska-type complexes have been characterized by X-ray crystallography and shown to possess the "para" orientation of added groups. Binding of these two groups to the fullerene results in an elongation of the fullerene along the axis between the two iridium complexes. The orientation of the added iridium complexes is the same as seen for both crystallographically identified forms of $C_{60}\{Ir(CO)Cl(PMe_2Ph)_2\}_2$. All four of these examples of crystalline "para" adducts of the type $C_{60}\{Ir(CO)Cl(PR_3)_2\}_2$ show very limited solubility in the solvent (benzene) from which they were grown.

The spectroscopic data for solutions of $C_{60}\{Ir(CO)Cl(PEt_3)_2\}_2$ in *o*-dichlorobenzene/toluene indicate that there is extensive dissociation in this solution and that a variety of isomeric forms of the double addition product coexist at low temperatures. At or near room temperature where the crystallization process occurs, the equilibria among the various adducts and their individual precursors are dynamic (as seen in the line widths in trace A of Figure 6). Thus, solubility and the process of crystal growth play major roles in the determination of which isomeric form is present in the solid state. In general, the high symmetry and low polarity of these "para" double addition products appear to contribute to their low solubility. Other examples of "para" double addition products, $C_{60}\{O_2OsO_2(py)_2\}_2$[15] and $C_{60}\{C(COOEt)_2\}_2$,[2] are also reported to have lower solubilities than their other regioisomers. Similarly, the successful crystallization of $C_{60}\{Ir_2Cl_2(\eta^4\text{-}C_8H_{12})_2\}_2{\cdot}2C_6H_6$, which has two dimeric iridium complexes bound at opposite ends of the fullerene, may result from preferential crystallization of a high-symmetry adduct with low solubility.[16] The reversible dissociation of $Pt(PR_3)_2$ units from complexes of the type $(C_{60})\{Pt(PR_3)_2\}_n$ has also been noted and cited as a factor which contributes to the crystallization of the highly symmetric form of $(C_{60})\{Pt(PR_3)_2\}_6$.[17]

Table 4. Crystal Structure Data

	compound	
	$C_{60}\{Ir(CO)Cl(PMe_3)_2\}_2{\cdot}2C_6H_6$	$C_{60}\{Ir(CO)Cl(PEt_3)_2\}_2{\cdot}C_6H_6$
formula	$C_{86}H_{48}Cl_2Ir_2O_2P_4$	$C_{92}H_{66}Cl_2Ir_2O_2P_4$
fw	1692.42	1782.63
system, space group	orthorhombic, *Cmcm*	monoclinic, *I2/a*
a, Å	20.188(4)	20.105(2)
b, Å	16.042(3)	12.4670(10)
c, Å	18.517(4)	26.458(2)
α, deg	90	90
β, deg	90	99.630(8)
γ, deg	90	90
V, Å^3	5997(2)	6538.2(10)
Z	4	4
T, K	123(2)	123(2)
radiation; *λ*, Å	Mo Kα; 0.710 73	Cu Kα; 1.541 78
μ, mm^{-1}	4.688	9.894
d_{calc}, Mg/m^3	1.875	1.811
transm factors	0.57−0.73	0.44−0.61
no. of reflcns	3641	4275
no. of reflcns ($I > 2\sigma(I)$)	2506	3987
params	225	242
R^a	0.065	0.072
w$R2^b$	0.1419	0.190

$^a R = \sum||F_o| - |F_c||/\sum|F_o|$, for $I > 2\sigma(I)$. ^{b} wR2 $= \sum[w(F_o^2 - F_c^2)^2]/\sum[w(F_o^2)^2]^{1/2}$.

Experimental Section

Preparation of Compounds. C_{60} was prepared by the arc vaporization of graphite[18] and purified by column chromatography on alumina.

$C_{60}\{Ir(CO)Cl(PMe_3)_2\}_2{\cdot}2C_6H_6$. Under a dioxygen-free atmosphere of dinitrogen, 114 mg (0.28 mmol) of $Ir(CO)Cl(PMe_3)_2$ was added to a solution of 20 mg (0.028 mmol) of C_{60} that was dissolved in 15 mL of benzene. The deep green solution was filtered and allowed to stand undisturbed for 7 days. The purple-black crystals that formed were collected by filtration and washed with benzene: yield 33 mg, 70% based on C_{60}. Crystals formed in this fashion were suitable for the single crystal X-ray diffraction study.

$C_{60}\{Ir(CO)Cl(PEt_3)_2\}_2{\cdot}C_6H_6$. As described above, 138 mg (0.28 mmol) of $Ir(CO)Cl\text{-}(PEt_3)_2$ was added to 20 mg (0.028 mmol) of C_{60} that was dissolved in 15 mL of benzene. After filtration, the green solution was allowed to stand undisturbed for seven days. The purple-black crystals that formed were collected by filtration and washed with benzene to give 35 mg (70% yield based on C_{60}) of product. Under microscopic examination the product appeared homogeneous, and crystals suitable for X-ray crystallography were obtained.

X-ray Data Collection. A suitable crystal of $C_{60}\{Ir(CO)Cl(PMe_3)_2\}_2{\cdot}2C_6H_6$ was coated with a light hydrocarbon oil and mounted in the 123(2) K dinitrogen stream of a Syntex $P2_1$ diffractometer that was equipped with a locally modified LT-1 low-temperature apparatus.

(15) Hawkins, J. M.; Meyer, A.; Lewis, T. A.; Bunz, U.; Nunlist, R.; Ball, G. E.; Ebbesen, T. W.; Tanigaki, K. *J. Am. Chem. Soc.* **1992**, *114*, 7954.
(16) Rasinkangas, M.; Pakkanen, T. T.; Pakkanen, T. A.; Ahlgrén, M.; Rouvinen, J. *J. Am. Chem. Soc.* **1993**, *115*, 4901.
(17) Fagan, P. J.; Calabrese, J. C. *Acc. Chem. Res.* **1992**, *25*, 134
(18) Haufler, R. E.; Conceicao, J.; Chibante, L. P. F.; Chai, Y.; Byrne, N. E.; Flanagan, S.; Haley, M. M.; O'Brien, S. C.; Pan, C.; Xiao, Z.; Billups, W. E.; Ciufolini, M. A.; Hauge, R. H.; Margrave, J. L.; Wilson, L. J.; Curl, R. F.; Smalley, R. E. *J. Phys. Chem.* **1990**, *94*, 8634.

Intensity data were collected with graphite-monochromated Mo Kα radiation. A crystal of $C_{60}\{Ir(CO)Cl(PEt_3)_2\}_2$ was handled similarly and mounted in the cold dinitrogen stream (at 123(2) K) of a Siemens P4/RA diffractometer which was equipped with a locally modified LT-2 low temperature device. Intensity data were collected with nickel-filtered Cu Kα radiation from a Siemens rotating anode X-ray generator that operated at 15 kW. Crystal data are given in Table 4. Two check reflections showed only random (<2%) variation in intensity during data collection. The data were corrected for Lorentz and polarization effects. Further details are given in the supplementary material.

Structure Solutions and Refinements. Calculations were performed with SHELXTL Plus (Sheldrick, Siemens, 1990). Scattering factors and corrections for anomalous dispersion were taken from a standard source.[19] Absorption corrections were applied to both structures with the program XABS2 which calculates 24 coefficients from a least-squares fit of (1/A vs. $\sin^2(\theta)$) to a cubic equation in $\sin^2(\theta)$ by minimization of F_o^2 and F_c^2 differences.[20] Each structure was solved by direct methods. Hydrogen atoms were fixed to appropriate carbon atoms though the use of a riding model with a fixed, isotropic U. For $C_{60}\{Ir(CO)Cl(PMe_3)_2\}_2{\cdot}2C_6H_6$ the iridium and phosphorus atoms, the chlorine atom in both major and minor orientations, the fullerene carbon atoms, and the trimethylphosphine carbon atoms were refined with anisotropic thermal parameters. The largest features in the final difference map were 1.03 Å from Ir and are probably absorption artifacts. For $C_{60}\{Ir(CO)Cl(PEt_3)_2\}_2$, only the iridium, chlorine, and phosphorus atoms were refined with anisotropic thermal parameters. The ethyl groups that involve C(36), C(37), C(40), and C(41) are ordered, while the other four ethyl groups show evidence of disorder that involves two alternate locations.

Acknowledgment. We thank the National Science Foundation (Grants CHE9022909 and CHE9321257) for support and Johnson Matthey, Inc., for a loan of iridium chloride.

Supplementary Material Available: Tables of crystal parameters, bond distances, bond angles, anisotropic thermal parameters, and hydrogen atom positions and U values for $C_{60}\{Ir(CO)Cl(PMe_3)_2\}_2{\cdot}2C_6H_6$ and $C_{60}\{Ir(CO)Cl(PEt_3)_2\}_2{\cdot}C_6H_6$ and a stereoview that shows the ethyl group disorder in $C_{60}\{Ir(CO)Cl(PEt_3)_2\}_2{\cdot}C_6H_6$ (18 pages). Ordering information is given on any current masthead page.

(19) *International Tables for X-ray Crystallography*; D. Reidel Publishing Co.: Boston, MA, 1992; Vol. C.
(20) Parkin, S. P. Ph.D. Thesis, University of California, Davis, CA, 1993.